Migration pathways in Ag-based superionic glasses and crystals investigated by the bond valence method

Stefan Adams
MKI, Universität Göttingen, Goldschmidtstraße 1, D-37077 Göttingen, Germany

Jan Swenson
Department of Applied Physics, Chalmers University of Technology, S-412 96 Göteborg, Sweden
(Received 24 May 2000; published 28 December 2000)

The bond valence technique has been applied on reverse Monte Carlo produced structural models of Ag-based superionic glasses and crystals. The results for the $(AgI)_{0.75}$-$(Ag_2MoO_4)_{0.25}$ and $(AgI)_{0.6}$-$(Ag_2O\text{-}2B_2O_3)_{0.4}$ glasses show the importance of including Ag sites with a high oxide coordination for the long-range mobility. The majority of the Ag^+ ions belonging to the long-range conduction pathways is coordinated to both O and I^-, and the pathways including only iodide coordinated sites are restricted to very local regions of a few Å. The most important finding of the present study is that the ionic conductivity as well as its activation energy can be determined directly from the ''pathway volume'' (i.e., the volume fraction of the percolating pathway cluster) of the structural models. The conductivity pathway volume relation is found to hold for glassy and crystalline conductors (including their temperature dependencies), whose conductivities differ by more than 11 orders of magnitude.

DOI: 10.1103/PhysRevB.63.054201 PACS number(s): 61.43.Fs, 66.30.Hs, 66.30.Dn

I. INTRODUCTION

Superionic solids show the remarkable behavior of a selective mobility in an otherwise frozen glass matrix. Apart from a few crystalline materials such as Rb_4AgI_5, the highest ionic conductivity at room temperature (up to nearly 10^{-1} S/cm) has been observed in AgI-doped glasses. The glasses are also better suited for technological applications (e.g., as solid electrolyte in electrochemical devices such as batteries, sensors, ''smart windows,'' etc.), due to their ease of preparation, their stability, and the large available composition ranges. However, despite a comprehensive experimental and theoretical effort the conduction mechanism is still not fully understood.[1] This is partly due to an incomplete knowledge of the microscopic structure, especially of the distribution and local environment of the mobile cations, which contain information about the most likely migration pathways.

Several models based on various hypothetical microscopic structures have been proposed to explain the high conductivities of superionic glasses. In one kind, the cluster model,[2–6] it is proposed that the metal halide salt is introduced into the amorphous network in clusters or micro domains of size >10 Å. Within the microdomains, which are assumed to have an internal structure similar to that of the dopant salt, the barriers for conduction are low, whereas there may be relatively large barriers between clusters. This model has been used particularly to explain the high ionic conductivity in AgI-doped glasses. AgI is, in its crystalline α phase above 147 °C, one of the best ionic conductors known. In another kind of model the ionic conductivity takes place within connected conduction pathways of relatively low activation barriers.[7–9] This idea was first proposed to explain the conductivity of metal-oxide modified oxide glasses and has later been extended in various forms to the salt doped glasses. The pathways are then assumed to be formed by the anions of the dopant salt and/or the negatively charged centers of the network, e.g., the BO_4^- groups in borate glasses. There are also various models which rest on the assumption that the ions of the dopant salt are effectively homogeneously distributed in the glass. Three of these are the random site model,[10] the dynamic structure model,[11–13] and the weak electrolyte model.[14–16] Although they rest on the same structural assumption these models are distinctly different. For example, in the random site model and the dynamic structure model all cations are assumed to contribute to the conductivity, whereas in the weak electrolyte model it is proposed that only a fraction of the cations contribute to the conduction. Furthermore, it has been suggested that the precise microscopic structure should be of subordinated importance and that the most important property for high conductivity is an open structure with large excess free volume.[17,18]

Experimentally, considerable effort has been made to establish a link between the microscopic structure and ionic conductivity in glasses. For this purpose it is important to determine both the local environment of the cations and the nature of the conduction pathways built up by the anions and the frozen glass matrix. In this paper we have applied the bond valence technique on reverse Monte Carlo (RMC) (Ref. 19) produced structural models of Ag-based superionic glasses and crystals. For highly AgI-doped glasses we show that the majority of the Ag^+ ions that contribute to the dc conductivity has a mixed oxide and iodide coordination. Furthermore, using the bond valence method, we are able to predict the dc conductivity of Ag-based glassy and crystalline conductors, whose conductivities differ by more than 11 orders of magnitude, directly from the RMC produced structural models, as was shown in a recent letter.[20]

II. BOND VALENCE MODELS FOR CONDUCTION PATHWAYS

The calculation of bond valence sums V has become a standard tool in crystallography to check the plausibility of a

proposed crystal structure or to localize light elements (H, Li) from x-ray-diffraction data.[21–23] Since many stable compounds are almost densely packed, sites with the matching valence often form well defined minima in these bond valence maps.

The total bond valence sum V of a silver ion in a glass can be expressed as

$$V=\sum_X S_{\text{Ag-}X}, \tag{1}$$

where the individual bond valences $S_{\text{Ag-}X}$ of bonds to all adjacent anions X are calculated employing tabulated empirical bond-length bond valence parameter sets (see, e.g., Refs. 24–27) mostly of the type

$$S_{\text{Ag-}X}=\exp\left[\frac{R_0-R_{\text{Ag-}X}}{b_0}\right]. \tag{2}$$

We have chosen the parameter set by Radaev, Fink, and Trömel,[26] given by

$$S_{\text{Ag-O}}=\exp\left[\frac{1.89\,\text{Å}-R_{\text{Ag-O}}}{0.33\,\text{Å}}\right], \tag{3a}$$

$$S_{\text{Ag-I}}=\exp\left[\frac{2.08\,\text{Å}-R_{\text{Ag-I}}}{0.53\,\text{Å}}\right], \tag{3b}$$

because it includes the influence of higher coordination shells, whereas the other parameter sets are generally based on the assumption that the bond valence sum should contain only contributions from bonds to the first coordination shell. Although this postulate can certainly not be applied to the calculation of bond valence maps, any of the mentioned literature parameters sets yields comparable bond valence isosurfaces after a proper renormalization of the valence sums.

Moreover, the denominator b_0 in the exponent expresses a relative measure for the different polarizabilities of the anions in Radaev's parameter set, whereas it is treated as a universal constant $b_0=0.37$ Å in most other parameter sets. Figure 1 demonstrates that the bond valence pseudopotentials that result from the parameters listed in Eq. (3) visualize the softness of Ag-I bonds.

Our three-dimensional bond valence maps are constructed by summing up bond valence contributions to all anions up to a distance of 8 Å for any point of a three-dimensional grid. Grid points at a distance to other cations M^+ smaller than the sum of radii[28] of Ag^+ and M^+ are treated as inaccessible. In Fig. 2 the bond valence isosurface for α-AgI is shown as an example.

Garrett *et al.*[29] demonstrated that such maps may equally serve to model the migration pathways of mobile ions in solid electrolytes. The basic assumption of this approach is that the ion transport from one equilibrium site to the next one follows pathways along which the valence mismatch $\Delta V=|V-V_{\text{ideal}}|$ remains as small as possible. In densely packed systems these are the pathways along which the bond valence sum remains as small as possible. For open crystal structures such as zeolites it means that guest cations will not reside at the center of large channels but will generally prefer to move along the walls of the channels.

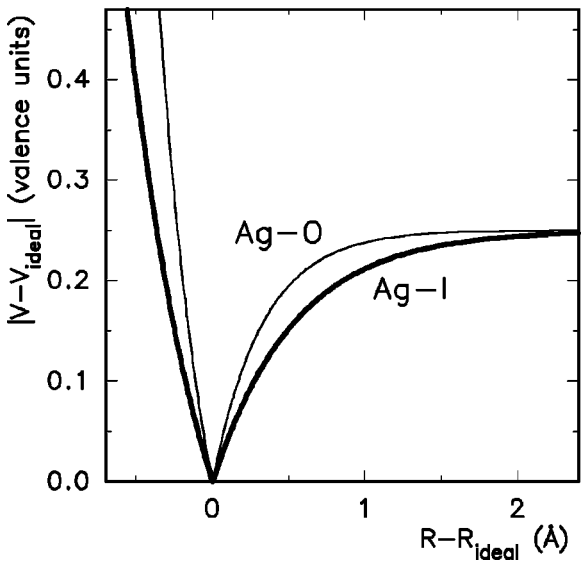

FIG. 1. Bond valence sum deviation $|V-V_{\text{ideal}}|$ resulting from the stretching of a single Ag-X bond for a tetrahedrally coordinated Ag-X (X=I,O).

As a first simple example, Garrett *et al.*[29] had demonstrated the equivalence of the bond valence pathways in α-AgI with pathways determined experimentally from an anharmonic atomic displacement refinement of neutron-diffraction data.[30] A recent similar study confirmed their result for $RbAg_4I_5$.[31]

In the meanwhile the ion transport in a variety of crystalline ion conducting systems has been investigated by the bond valence technique (see, e.g., Refs. 32–38). Three-dimensional graphical representations of isosurfaces with constant bond valence mismatch like the ones in Fig. 2 provide a vivid image of the pathway topology. Still additional information (e.g., on the occupancy of the cation sites and

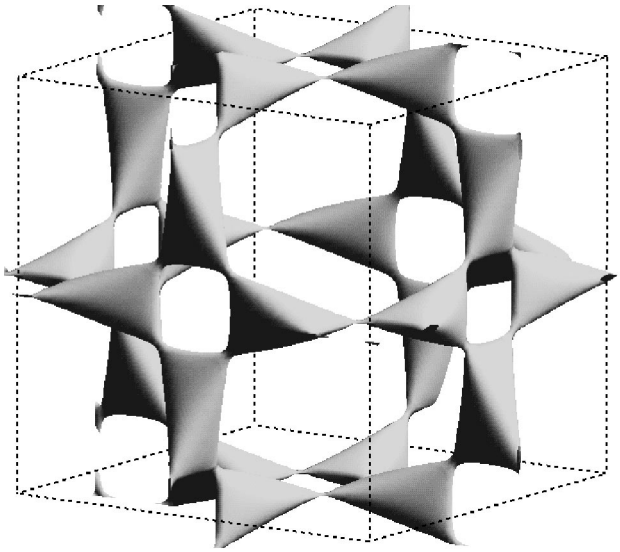

FIG. 2. Bond valence isosurface for α-AgI ($\Delta V=0.05$).

the jump distances) is generally required to derive a transport mechanism from such a bond valence study.

Strictly speaking an application of the bond valence method to determine pathways of mobile ions requires a local model of the immobile part of the structure. For crystalline ionic conductors with a minor degree of disorder the crystallographically determined time- and space-averaged structure is often a sufficient approximation to the characteristic local coordinations. In these systems it is found that the minimum value of the valence interval $V \pm \Delta V$, at which the bond valence isosurface for a mobile ion forms an infinite network including occupied sites, is related to the activation energy.[38] For superionic systems with their generally high degree of disorder the crystallographic structure information yields only an averaged information, from which the actual local coordinations of the mobile ions have to be derived, e.g., by force field calculations.[33]

The simplicity of the bond valence approach keeps comparatively large systems manageable so that the bond valence method is well suited to investigate the ionic conduction in comparatively large model systems and hence also in glassy ion conductors, provided that the local coordination for the mobile ions is known. Previously we had combined the bond valence approach with molecular mechanics and snapshots from molecular-dynamics simulations of highly disordered systems.[33] In that case starting models for the local structure have to be derived from the crystal structure of related compounds (e.g., crystalline silver iodide silver oxyacid salts).[32,33,39,40] In this work a more direct approach is chosen, the combination of the bond valence technique with reverse Monte Carlo (RMC) modeling.[19]

III. COMBINATION OF RMC WITH THE BOND VALENCE APPROACH

The reverse Monte Carlo technique[19,41,42] models the structure of disordered materials by fitting a structural model to experimental data from neutron and/or x-ray diffraction, extended x-ray-absorption fine structure (EXAFS), etc., using a standard Metropolis[43] Monte Carlo algorithm, where the minimized quantity is not the energy of the system but the squared difference between the calculated and experimental structure factors. For the present study, neutron structure factors over a large Q range ($0.2-50$ Å^{-1}) were determined with the wide-angle time-of-flight liquid and amorphous materials diffractometer (LAD) (Ref. 44) at the pulsed neutron source ISIS, Rutherford-Appleton Laboratory. The corresponding x-ray data were collected using the high-precision powder diffractometer station 9.1 at SERC's Synchrotron Radiation Source, Daresbury Laboratory, UK.[45]

In contrast to molecular dynamics (MD) or other simulation techniques, the RMC, thus is virtually a modeling technique, which is based on experimental data. Thereby RMC models, e.g., correspond to the temperature of the sample in the underlying measurements. The resulting RMC models may be roughly conceived as snapshots of the modeled systems. Thermal vibration of each atom is accounted for in these models, not extracted as time-averaged quantities such as Debye-Waller terms but in the form of local bond stretching and bending of equivalent particles in different parts of the model.

Thus a RMC produced model should provide the essential structural features characterizing the system under study. Still RMC models should not be misunderstood as depicting the atomic distribution within the sample in every detail. Previous studies have shown that without using certain constraints based on chemical knowledge, the RMC method is not likely to produce physically sensible structural models.[46] RMC tends to produce the most disordered structure that is consistent with the experimental data and the constraints, i.e., the configurational entropy is maximized. However, the number of possibilities to fit the data will be significantly reduced using appropriate constraints and the final structural model is likely to be much more realistic. The constraints we used were of three kinds; closest atom-atom approach, connectivity, and bond valence sum. The closest distances that two atoms were allowed to approach were determined from the experimental diffraction results, e.g., the pair-correlation function and ionic radii. The connectivity constraints were usually based on NMR data[47] and used within the glass network (e.g., between the B and O atoms or within the MoO_4^{2-} and WO_4^{2-} molecular ions) to ensure that the atoms are linked together properly. More details on the connectivity constraints that have been applied for the present RMC produced models are given in Refs. 48–52. The third kind of constraint, based on the above-mentioned bond valence sum method, is a simple way to introduce chemical information into the local coordination of the mobile Ag^+ ions. Such a soft constraint minimizes the valence deviation from $V(\mathrm{Ag})_{\mathrm{ideal}}=1$ for each Ag^+ ion and thereby reduces the number of unphysical Ag coordinations.

The interpretation of bond valence isosurfaces in these RMC models or any models for disordered or amorphous systems necessarily differs from studies of crystalline systems, where the primary aim is a detailed description of a limited number of crucial elementary migration barriers between the equilibrium sites of the mobile species. The number of potentially relevant migration barriers in real glasses is infinite and even in our RMC models, typically consisting of 4000 atoms, a description of arbitrarily selected migration barriers might be misleading. Visual inspection of the bond valence isosurfaces may provide a first qualitative impression. Quantitative information on the total system can only be extracted by a statistical description of the total bond valence isosurface, employing, e.g., procedures adopted from percolation theory.

The three-dimensional grid used to calculate the valence sums separates the modeled box into ca. 4 million cubic volume elements corresponding to a size of $(0.2-0.3$ Å$)^3$ per volume element. Such a volume element is treated as accessible to mobile Ag^+ ions, if the valence sum for a hypothetical Ag^+ at the ''grid point,'' i.e., at the center of the volume element, lies within a valence interval $V_{\mathrm{ideal}} \pm \Delta V$ or if the valence mismatch ΔV changes its sign within the volume element. The second criterion has been added to cushion the effects from the limited resolution of our grid. Accessible volume elements that share common faces or edges belong to the same ''pathway cluster.''

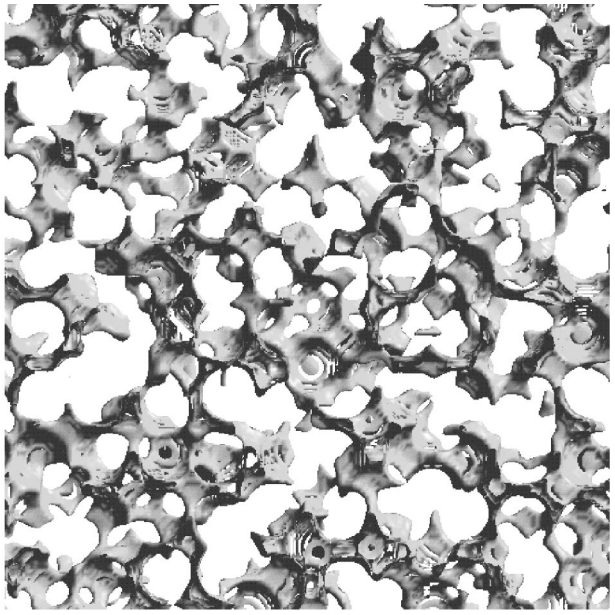

FIG. 3. Bond valence isosurface for a RMC model of α-AgI at $T=525$ K.

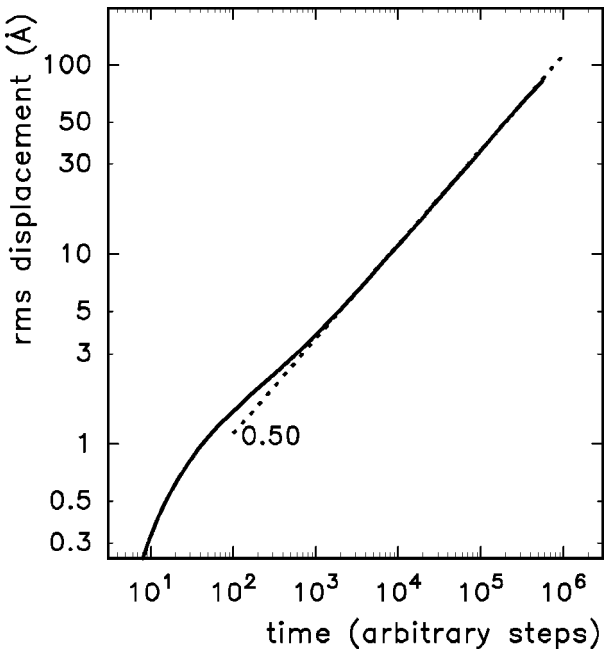

FIG. 4. Simulated time dependence of the root-mean-square displacement for mobile Ag^+ ions within the bond valence pathway of α-AgI.

IV. RESULTS

A. Conduction pathways in RMC models of *a*-AgI

In order to explore the feasibility of extracting information on the pathway topology and ion mobility from such RMC models, we first investigated RMC models of α-AgI at 525 and 740 K.[48] The characteristic motifs and translational symmetry of the bond valence pathways in α-AgI, determined from its crystal structure (cf. Fig. 2), remain clearly recognizable in the bond valence isosurfaces for the RMC model shown in Fig. 3.

Due to the snapshot character of the RMC models the local distortions give rise to an average valence of the Ag sites, that lies somewhat below the equilibrium value $V(\mathrm{Ag})_{\mathrm{ideal}}=1.00$. For the α-AgI RMC models we found $\overline{V}(\mathrm{Ag})=0.88$ and at 740 K the average Ag valence even drops to 0.85. The isosurface for $V=1.00$ provides an infinite pathway through the whole modeled box. This means that for the RMC models there is no such simple correlation between the valence mismatch and the activation energy of the transport steps as for the energy-minimized models derived from crystal structures.[38] Still the concurrent topology of the Ag bond valence isosurfaces in crystal structures and corresponding RMC models demonstrate the feasibility of the chosen approach. Moreover the slight increase of the conductivity from 525 to 740 K is accompanied by an increase of the volume fraction of the ''infinite pathway cluster'' from 7.6 to 8.0%. For both models this infinite cluster contains 99.7% of all ''accessible'' grid points.

The relevance of the bond valence isosurfaces from RMC models has been further examined by a Monte-Carlo-like simulation of the Ag^+ motion through the system as hops from one grid-point to the next one at a distance of 0.2–0.3 Å. Successful jumps require that the valence at the target grid point lies in the range 1.00 ± 0.05. $\Delta V=0.05$ has been chosen as the valence mismatch threshold, because it equals the minimum valence mismatch for which pathways in the crystal-structure-model of α-AgI become infinite. These random walks were repeated using all ''mobile'' Ag^+ as starting points, that means all modeled Ag^+ positions with the matching valence sum ($\approx$37% of all Ag^+). The shape of the log-log diagram of the root-mean-square (rms) displacement vs pseudotime steps (Fig. 4) averaged over all mobile Ag ions appears quite plausible: The initial steep rise for low values of the rms displacement corresponds to unrestricted local vibrations within the same energy minimum. As the rms displacement approaches the distance between equilibrium sites ($\approx$2 Å in α-AgI) the slope distinctly decreases, since only a small fraction of the local hops leads into an adjacent equilibrium site. On larger length scales the model systems behaves homogeneously, so that the rms displacement increase becomes proportional to $t^{1/2}$ in accordance to the diffusion law. The exponent $\frac{1}{2}$ suggests that the connectivity of the conduction pathway network is considerably above the percolation threshold. A more detailed discussion of these diffusion simulations for α-AgI as well as a comparison to analogous computations for several silver ion conducting glasses will be published elsewhere.[52]

B. Ag conduction pathways in RMC models of silver ion conducting glasses

The involvement of Ag^+ ions with mixed oxide-iodide coordination in the long-range Ag^+ conduction of AgI-doped fast ion conducting glasses is still a matter of discussion.[2–6,50,53–56] The bond valence approach should be well suited to provide new insight about this issue. For this purpose we chose the systems $(AgI)_{0.75}$-$(Ag_2MoO_4)_{0.25}$ (Ref.

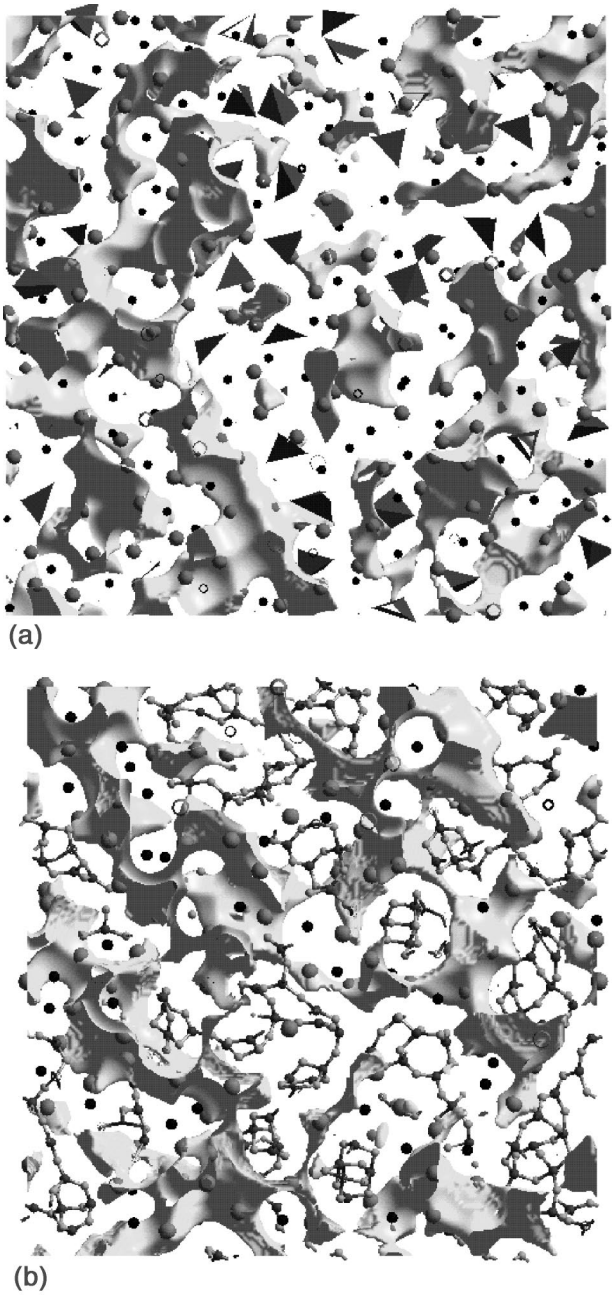

FIG. 5. 5-Å-thick slices through bond valence isosurfaces for RMC models of the glassy phases (a) $(AgI)_{0.75}$-$(Ag_2MoO_4)_{0.25}$ and (b) $(AgI)_{0.6}$-$(Ag_2O\text{-}2B_2O_3)_{0.4}$ Ag: large gray spheres; I: black spheres, molybdate as tetrahedra, borate shown as a network with small spheres for B (dark gray) and O (light gray).

49) and $(AgI)_{0.6}$-$(Ag_2O\text{-}2B_2O_3)_{0.4}$ (Ref. 50) as representative model systems for molecular and network glasses, respectively. As for α-AgI each of the model systems contained approximately 4000 atoms with periodic boundary conditions.

Slices through the bond valence isosurfaces for the two glassy systems are shown in Fig. 5. At first sight the complex isosurfaces may look rather puzzling, since there is no more translational order except for the periodic boundary conditions.

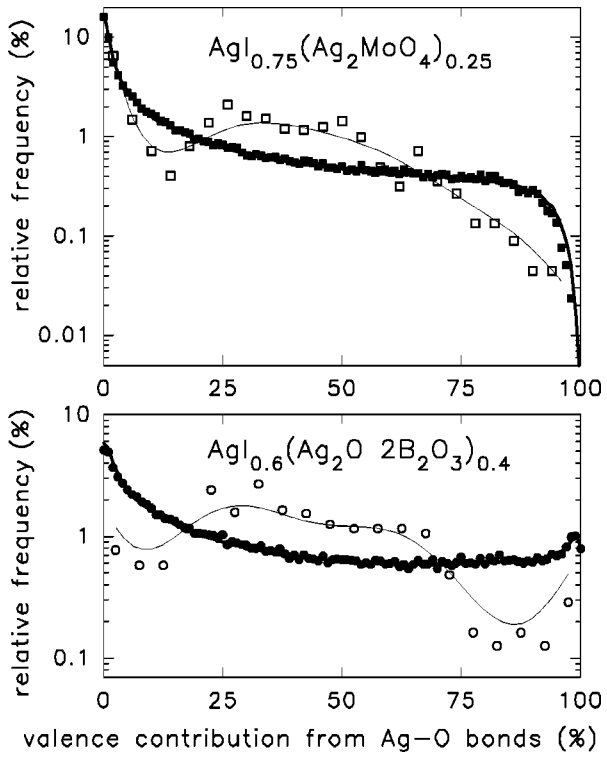

FIG. 6. Occurrence of sites with a certain oxide contribution to the total Ag valence sum: (filled symbols refer to all grid points with $V=1.00\pm0.05$, open symbols to the Ag sites with $V=1.00\pm0.05$ of the RMC model). The solid lines indicate the corresponding behavior for all grid points/all Ag sites irrespective of their valence mismatch.

For each model system the mean fraction of the valence sum that originates from bonds to oxide ions harmonizes with the respective overall iodide/oxide ratio both for an averaging over all grid points and over all Ag^+ positions. A more detailed picture of the characteristic features of both systems is obtained from the distribution of volume elements with different oxide contributions displayed in Fig. 6.

Due to the high iodide content of the system $(AgI)_{0.75}$-$(Ag_2MoO_4)_{0.25}$, purely iodide coordinated sites constitute a non-negligible portion of the conduction pathways and for higher oxide contributions the number of sites decreases monotonically. While the general trend is similar for the borate system, its lower iodide content results in a more balanced distribution as a function of the oxide contribution. For both glasses the vast majority of the volume elements in the conduction pathways (full symbols) occupies positions with a mixed coordination. The distribution of the oxide contributions for the modeled Ag^+ positions (hollow symbols) deviates from the relative frequency of the volume elements. In both glasses, positions where bonds to oxide ions provide about 20 up to 70% of the total valence sum appear to be slightly favored in comparison to the frequency of their occurrence in the grid. In view of the low number of Ag^+ ions with pure oxide coordinations, data for the range above 75% can only be raw estimates.

As anticipated from the distribution of the coordination types in the modeled systems, the assumption that only Ag^+

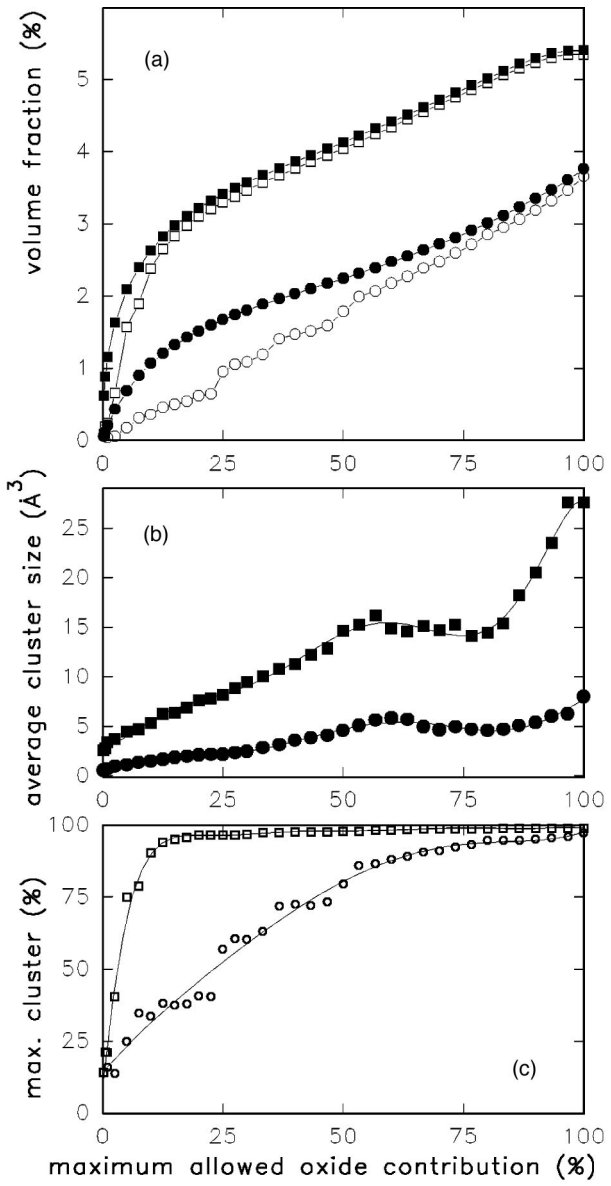

FIG. 7. Variation of (a) the volume fraction of accessible sites (full symbols) or of the maximum cluster (open symbols), (b) the average cluster-size, and (c) the fraction of accessible sites belonging to the maximum cluster as a function of the maximum allowed oxide contribution to the total Ag valence. Squares refer to the system $(AgI)_{0.75}$-$(Ag_2MoO_4)_{0.25}$, circles to $(AgI)_{0.6}$-$(Ag_2O$-$2B_2O_3)_{0.4}$.

ions with a pure iodide coordination or up to a certain oxide fraction of the coordination contribute to the ionic conductivity drastically affects the volume of the conduction pathways. The effects are quantified in Fig. 7(a) where the volume fraction of accessible sites is shown as a function of the maximum allowed oxide contribution to the Ag bond valence. Figure 7(b) reveals that for the molybdate glass the average size of the pathway clusters increases linearly by a factor of ≈ 5 if the maximum allowed oxide fraction is increased from 0 to 50%. The small number of sites with a predominant oxide coordination might be of minor importance for the volume of the pathways. Nevertheless the average size of the pathway clusters is significantly raised by the assumption that all the grid points with the matching valence may belong to the transport pathways irrespective of the type of coordinating anions. The final increase may be traced back to the attachment of many small isolated clusters to the infinite cluster. Our findings fairly agree with the results of a molecular-dynamics study on AgI-Ag_2MoO_4 glasses by Karthikeyan and Rao.[53]

Peculiarities of the molybdate and borate glasses are highlighted in Fig. 7(c). For the molybdate system, the fraction of the accessible grid points that are part of the maximum cluster (and thereby may contribute to a long-range charge transport) rises steeply with the maximum permitted oxide fraction. The corresponding curve for the borate system increases only gradually with the maximum allowed oxide fraction suggesting that even predominantly oxide coordinated sites should play an important role. Thus typical conduction pathways in the borate system run along the internal surfaces of the borate network [cf. Fig. 5(b)]. In this sense the resulting conduction pathways bear some similarity to the earlier ''connective tissue model.'' [57]

A reduced volume fraction of the infinite cluster furthermore diminishes the connectivity of the conduction pathways network as the cluster-size approaches the percolation threshold. In the extreme case that only purely iodide coordinated Ag^+ ions were supposed to be mobile, all pathway clusters become finite, thereby restricting the mean displacement of the ''mobile'' Ag^+ to about 3–4 Å. If only Ag^+ ions up to a certain oxide fraction of the valence sum, e.g., 25% were mobile, the pathway clusters become infinite for both systems, but due to the proximity to the percolation threshold the rms displacement increases only with t^γ, where the exponent γ is considerably $<\frac{1}{2}$. A detailed discussion of this aspect is in preparation.[52]

This general tendency is augmented by the clearly nonstatistical spatial distribution of differently coordinated volume elements. While this is self-evident for network glasses, it also holds for the molecular molybdate glass. As only a few percent of the grid points satisfy the bond valence criterion (1.5% in Ag_2O-$4B_2O_3$ up to 8% in α-AgI), the existence of infinite pathway clusters is in itself a proof of the nonrandom distribution. Figure 8 reveals the nature of this inhomogeneity for $(AgI)_{0.75}$-$(Ag_2MoO_4)_{0.25}$. The displayed iodide-coordinated local loops interconnected by predominantly oxide-coordinated sites seem to be a characteristic feature of the bond valence isosurfaces in AgI-AgM_xO_y glasses in accordance to observations reported for crystalline compounds with similar compositions.[32,33] This may be explained as an inherent consequence of the softness of the Ag-I potential: mobile Ag^+ ions in local voids tend to be rather iodide than oxide coordinated.

From the above considerations it is evident that silver ions with mixed coordinations must be involved in the transport process in the $(AgI)_{0.75}$-$(Ag_2MoO_4)_{0.25}$ glass. Our simulations of the Ag^+ ion transport by random walks within the bond valence pathway clusters provide a simple raw estimate of the local mobilities from the correlation between the rms displacement of a Ag^+ ion during very short periods of the simulation (e.g., 100 simulation time steps) and the

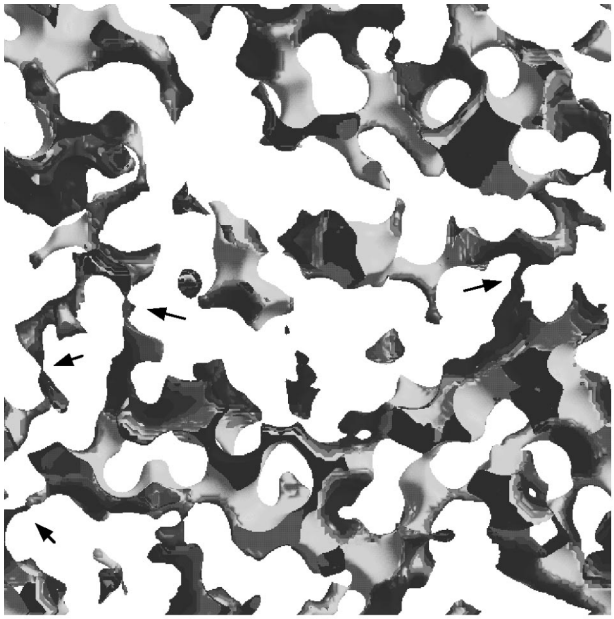

FIG. 8. 2-Å-thick slice through the bond valence pathway model of $(AgI)_{0.75}$-$(Ag_2MoO_4)_{0.25}$ for $\Delta V=0.05$ (box length 44.7 Å). Light parts of the pathway surface correspond to mainly iodide coordinated Ag^+ sites, while dark regions represent mainly oxide coordinated sites. Arrows indicate examples for bridges of predominantly oxygen coordinated sites connecting mainly iodine coordinated regions of the pathways.

coordination of the Ag^+ averaged over this time interval (expressed in terms of the relative oxide contribution to the bond valence sum). The resulting dependence of the local mobility on the oxide contribution to the total Ag valence in the glasses $(AgI)_{0.75}$-$(Ag_2MoO_4)_{0.25}$ and $(AgI)_{0.6}$-$(Ag_2O$-$2B_2O_3)_{0.4}$, as outlined in Fig. 9, suggests an only slightly decreasing local Ag^+ mobility of the Ag^+ for

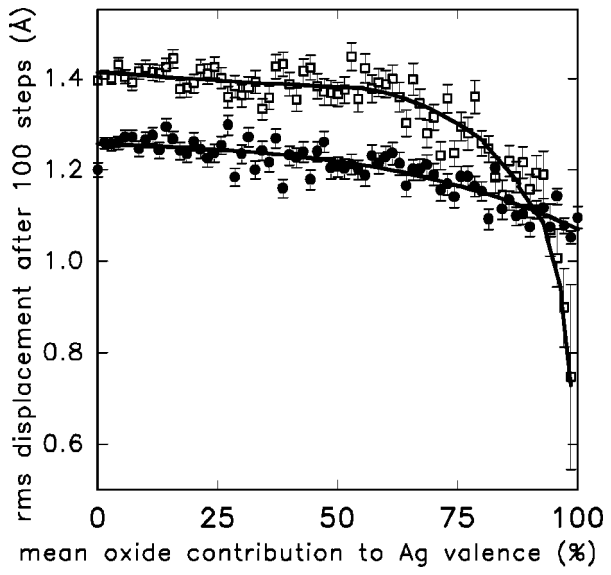

FIG. 9. Dependence of the Ag^+ mobility on the mean relative oxide contribution to the total valence for $(AgI)_{0.75}$-$(Ag_2MoO_4)_{0.25}$ (hollow squares) and $(AgI)_{0.6}$-$(Ag_2O$-$2B_2O_3)_{0.4}$ (full circles).

increasing oxide contribution to the coordination, except in the case of the molybdate glass, where the Ag^+ mobility decreases rapidly for oxide contributions $>90\%$. This oversimplifying approach should obviously only be taken as a qualitative, rather than quantitative, description of how the local mobility depends on the oxide contribution to the total Ag valence.

C. Structure-conductivity-correlation

As mentioned above, the RMC produced structural models refer to real samples and hence also to specific experimental conditions of the sample such as its temperature, pressure, etc., and consequently to a well-defined ionic conductivity. This might open a way to estimate the conductivity of a sample directly from the RMC model of its structure. For this purpose we investigated the bond valence pathway clusters of two further silver iodide silver oxyacid glasses $(AgI)_{0.75}$-$(Ag_2WO_4)_{0.25}$ and $(AgI)_{0.6}$-$(Ag_2O$-$B_2O_3)$ as well as two systems with lower conductivities, namely the two undoped borate glasses Ag_2O-$2B_2O_3$ and Ag_2O-$4B_2O_3$.[49,51] The restriction of our study to glassy systems and cubic crystalline phases, which both behave isotropically with respect to the conductivity tensor, simplifies the ambitious task slightly.

The simplest property of the bond valence models that fundamentally affects the conductivity of the systems under study is obviously the volume fraction of the infinite conduction pathway cluster, as only the silver ions attached to the infinite cluster may contribute to the dc conductivity. Since ion transport is basically a one-dimensional process it may be more appropriate to relate the mobility of ions in a system to a one-dimensional feature of its structure model (such as a mean free path length for Ag^+ ions in the pathway cluster) and hence to the cube root of the pathway volume fraction.

A model-free determination of precise absolute values for the volume fraction of the long-range pathways is not possible, since the absolute volume fraction is obviously related to the criterion by which we decide whether a volume element should be counted as ''accessible.'' Although our choice of the valence interval $V\pm\Delta V=1.00\pm0.05$ was not arbitrary, it appears worthwhile to check before proceeding to what extent the volume fraction of the pathway clusters varies with the selected valence mismatch threshold ΔV. Fortunately it turns out that ΔV is not a critical quantity as we deal only with relative quantities to compare the properties of the different systems. Figure 10 illustrates the uniform variation of the volume fraction of the infinite cluster with the valence mismatch threshold ΔV for room-temperature models of $AgI_{0.75}$-$(Ag_2MoO_4)_{0.25}$, $(AgI)_{0.6}$-$(Ag_2O$-$2B_2O_3)_{0.4}$, Ag_2O-$2B_2O_3$, Ag_2O-$4B_2O_3$, and the two models of crystalline α-AgI at 525 and 740 K. The proportion between the volume fractions for different systems varies only slightly over a broad range of ΔV values. Even the assumption of a significant reduction of ΔV with increasing conductivity (in analogy to the reduction of the activation energy) would not alter the sequence of the phases. As there is presently no way

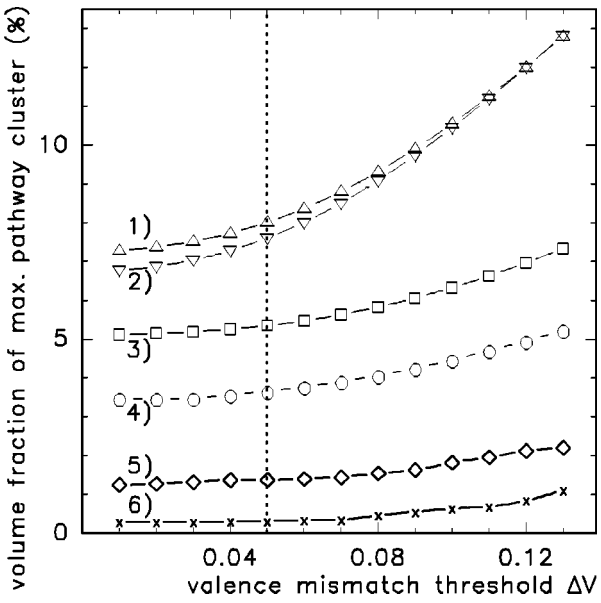

FIG. 10. Dependence of the volume fraction of the maximum Ag conduction pathway clusters on the selected valence mismatch threshold ΔV for the RMC models of crystalline AgI at 525 K (1) and at 740 K (2), of the silver iodide silver oxysalt glasses $(AgI)_{0.75}$-$(Ag_2MoO_4)_{0.25}$ (3) and $(AgI)_{0.6}$-$(Ag_2O\text{-}2B_2O_3)_{0.4}$ (4) as well as of the undoped borate glasses $Ag_2O\text{-}2B_2O_3$ (5) and $Ag_2O\text{-}4B_2O_3$ (6).

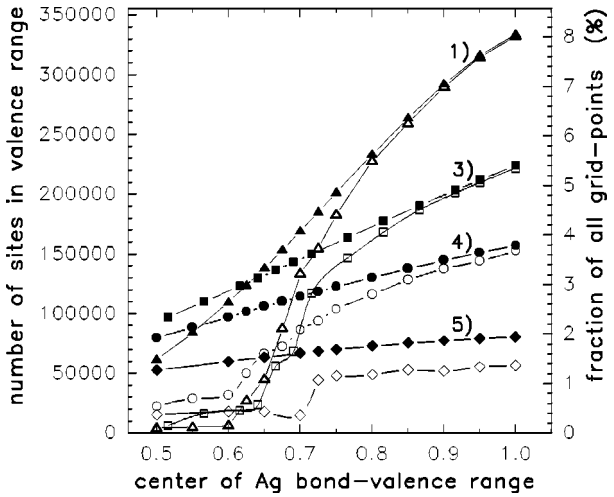

FIG. 11. Filled symbols: total number of grid points with a valence in the interval $V \pm 0.05$ for different choices of V in the investigated RMC models of Ag^+ conductors (numbers refer to the systems listed in Fig. 8). Open symbols represent grid points that form the infinite (or maximum) pathway cluster. The ratio between the volume fractions of the continuous pathway in different ion conductors changes only slightly with the choice of the bond valence interval.

of quantifying such a potential influence of the activation energy on ΔV a constant ΔV has been used in all further calculations.

The ideal valence for a silver ion in a relaxed structure model is obviously 1.00. Nevertheless, it has been supposed from the reduction of the average valence of Ag^+ ions in the RMC snapshots that the center of the valence interval should also be adapted to these average valences,[58] that lie in the range $0.8 < V < 0.92$ for our models. As demonstrated in Fig. 11, even a major shift of the valence interval produces only minor modifications of the ratio between the volume fractions of the investigated systems. Additionally, the variation of the pathway cluster size with the choice of the valence interval corroborates the previous statements on the pathway topology in these systems. For the investigated glasses a percolation threshold is discernible as a sudden drop of the maximum cluster size in the region $0.6 < V < 0.7$. For valences above this threshold the pathway becomes infinite, whereas lower valences occur only in localized voids. Owing to the small cluster volume in the undoped $Ag_2O\text{-}4B_2O_3$ glass the system remains close to the percolation threshold even for $V = 1$. Therefore we feel that the conductivity of this system roughly marks the lower limit of conductivities that can be modeled by our approach.

From the above arguments it may be concluded that — for a given choice of the valence interval $V \pm \Delta V$ — the ratio between the volume fractions of the maximum pathway clusters in different ion conductors provides a reliable tool for a comparison of the Ag^+ ion mobilities in these systems. Figure 12 reveals the existence of a remarkably strong novel correlation between the volume fraction of the maximum pathway cluster and the conductivity of the sample.[20] The relation shows that

$$\log(\sigma T) \propto \sqrt[3]{F_{\max\,\mathrm{clust}}}, \tag{4}$$

where $F_{\max\,\mathrm{clust}}$ denotes the volume fraction of the maximum pathway cluster. Conductivity data are taken from Refs. 36, 47, and 59–71.

This correlation is found to hold for systems whose conductivities differ by more than 11 orders of magnitude. The two data points 4 and 7 in Fig. 12, which refer to two independent RMC models of the same silver iodide doped borate glass, give an idea of the reproducibility of the volume fraction determination. Accordingly, the slight conductivity difference between the two models of pure α-AgI is correctly described.

Even bond valence isosurfaces, for which the local structure model is not a RMC model but a snapshot model from a molecular-dynamics (MD) simulation seem to obey the same relation reasonably well, as indicated by data point 10 in Fig. 12, that refers to a MD simulation of $Ag_{16}I_{12}P_2O_7$.[33] An obvious prerequisite for the extension of this correlation to other ion conducting systems would be the availability of a consistent set of bond valence parameters.

An estimate of the experimental activation energy for the ionic conduction E_σ may accordingly be derived from the structural model: $E_\sigma / k_B T$ equally varies linearly with the cube root of the bond valence pathway volume fraction F as shown in Fig. 13. In those systems for which several experimental determinations were reported, the presented correlation predicts activation energies within the range of the experimental scatter. A more detailed analysis would also have to include the partial compensation of the decreasing prob-

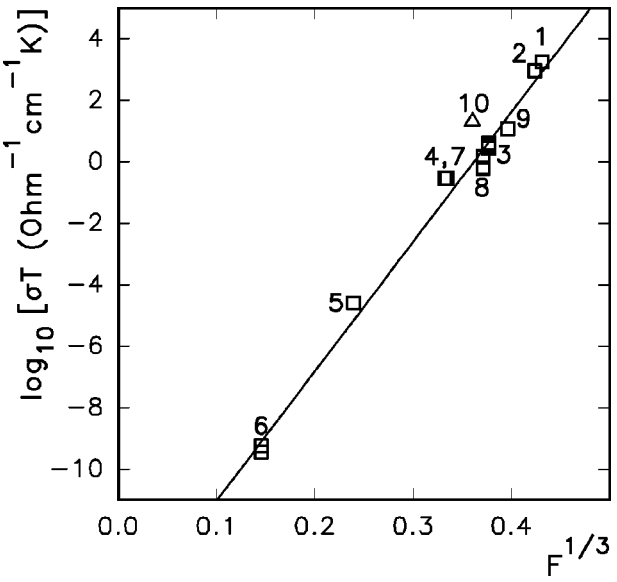

FIG. 12. Correlation between the experimental ionic conductivity σ and the volume fraction F of the infinite Ag conduction pathway clusters for the RMC models of crystalline AgI at 525 K (1) and at 740 K (2), of the silver iodide silver oxysalt glasses $(AgI)_{0.75}$-$(Ag_2MoO_4)_{0.25}$ (3), $(AgI)_{0.6}$-$(Ag_2O\text{-}2B_2O_3)_{0.4}$ (two models 4, 7), $(AgI)_{0.6}$-$(Ag_2O\text{-}2B_2O_3)_{0.4}$ (8) and $(AgI)_{0.75}$-$(Ag_2WO_4)_{0.25}$ (9), as well as of the undoped borate glasses $Ag_2O\text{-}2B_2O_3$ (5) and $Ag_2O\text{-}4B_2O_3$ (6). For comparison the result for a snapshot from a MD simulation of crystalline $Ag_{16}I_{12}P_2O_7$ is also included (10). Conductivity data are taken from Ref. 59 for (1, 2), Refs. 36, 60, and 61, for (3) Refs. 63 and 64 for (4–7), Refs. 66, 67, and 68 for (8) Ref. 69 for (9), and Refs. 70 and 71 for (10).

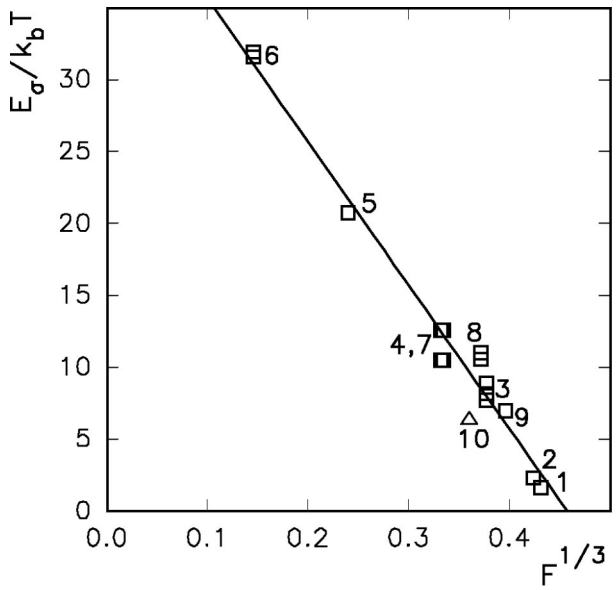

FIG. 13. Correlation between the experimental activation energy for ionic conductivity E_s and the volume fraction F of the infinite Ag conduction pathway clusters for the RMC models. Numbers refer to the same samples as in Fig. 1. Experimental data are taken from Ref. 59 for (1, 2), Refs. 36, 60, and 61 for (3) Refs. 47, 63, and 65 for (4–7), Refs. 66 and 68 for (8), Ref. 69 for (9), and Ref. 70 for (10).

ability of successful jumps by an increase in the attempt frequency with increasing activation energy. A crude estimate of the pre-exponential factor σ_0 may be derived from a combination of the two presented correlations. In accordance with the Meyer-Neldel rule[72] σ_0 is found to increase slightly with decreasing F.

These interesting structure-conductivity correlations bear some similarities to the basic idea of the ''free volume approach,'' [18] that the relative expansion of the network on doping should be related to the increase of the conductivity, given by

$$\frac{\sigma}{\sigma_0} = \left(\frac{V - V_0}{V_0}\right)^3, \tag{5}$$

where V denotes the volume per network atom and index 0 refers to the undoped glass system.

Obviously the reduced density of glasses when compared to their crystalline constituents is closely related to the existence of conduction pathways. The main advantage of relation (4) over Eq. (5) is that it is not restricted to salt doped glasses, it also predicts the conductivity of undoped glasses with completely different types of networks, as well as crystalline superionic phases. However, a structural model of the solid must be available in order to calculate the bond valence isosurface, while the knowledge of the sample density is sufficient to apply Eq. (5).

Here, we prefer the more physical term ''pathway volume'' over ''free volume.'' This is not only a change of the terminology. It emphasizes that the effect of the ''free volume'' is not independent of its spatial distribution and of the surrounding anions. A narrow channel will be more important to the total conductivity than a spherical void of the same volume. Our bond valence approach inherently accounts for that, as only the shell of such a sphere is counted as part of the pathway. Due to the different softness of the Ag-X potentials the thickness of this shell depends on the type of the neighboring anions illustrating why highly polarizable ions promote ionic conductivity.

In a real system conduction pathways are not fixed. Their detailed shape and location varies with thermal motion, but pathways of similar characteristics exist at any time somewhere in a macroscopic sample. It should also be noted that the volume of the conduction pathways is only one out of several quantities of relevance to the conductivity that may be extracted from the RMC models by means of the bond valence technique. Further example would be the fraction and mobility of ''mobile'' Ag^+ ions, i.e., of those Ag^+ ions with sufficiently small valence mismatches, which equally increase with the conductivity of the system.

V. CONCLUDING REMARKS

Bond valence models of ion conduction pathways may be utilized to elucidate the conduction mechanism and to estimate the conductivity of Ag^+ ion conductors. A structural model of the atomic structure is required to construct a pathway model (i.e., an infinite cluster of sites with matching Ag

bond valences). For structurally disordered ionic conductors such structural models may be derived from diffraction data, using the reverse Monte Carlo (RMC) method. We have used a modified RMC algorithm, which includes a soft constraint on the bond valence sum of each Ag^+ ion. This approach yields chemically meaningful structural models in quantitative agreement with the available diffraction data, which can be used to model ion conduction pathways. For all the investigated systems a simple correlation holds between the volume of the continuous isovalence pathway cluster and the ionic conductivity. In contrast to earlier *free volume* approaches this correlation includes the variation of conductivity and activation energy for different undoped oxide glasses as well as crystalline superionic phases.

ACKNOWLEDGMENTS

We are grateful to Dr. R. L. McGreevy and Dr. V. M. Nield for the RMC configurations of α-AgI at 525 and 740 K as well as to Professor L. Börjesson for experimental neutron-diffraction data on silver borate glasses. Financial support to J.S. from the Swedish Natural Science Research Council and to St.A. from the Deutsche Forschungsgemeinschaft is gratefully acknowledged.

[1] C. A. Angell, Annu. Rev. Phys. Chem. **43**, 693 (1992).
[2] M. Tachez, R. Mercier, J. P. Malugani, and A. J. Dianoux, Solid State Ionics **18–19**, 372 (1986).
[3] J. P. Malugani, M. Tachez, R. Mercier, A. J. Dianoux, and P. Chieux, Solid State Ionics **23**, 189 (1987).
[4] A. Fontana, F. Rocca, and M. P. Fontana, Phys. Rev. Lett. **58**, 503 (1987).
[5] C. Rousselot, M. Tachez, J. P. Malugani, R. Mercier, and P. Chieux, Solid State Ionics **44**, 151 (1991).
[6] C. Rousselot, J. P. Malugani, R. Mercier, M. Tachez, P. Chieux, A. J. Pappin, and M. D. Ingram, Solid State Ionics **78**, 211 (1995).
[7] G. Carini, M. Cutroni, A. Fontana, G. Mariotto, and F. Rocca, Phys. Rev. B **29**, 3567 (1984).
[8] T. Minami, J. Non-Cryst. Solids **73**, 273 (1985).
[9] G. N. Greaves, J. Non-Cryst. Solids **71**, 203 (1985).
[10] A. M. Glass and K. Nassau, J. Appl. Phys. **51**, 3756 (1980).
[11] P. Maass, A. Bunde, and M. D. Ingram, Phys. Rev. Lett. **68**, 3064 (1992).
[12] A. Bunde, M. D. Ingram, P. Maass, and K. L. Ngai, J. Non-Cryst. Solids **131–133**, 1109 (1991).
[13] A. Bunde, M. D. Ingram, and P. Maass, J. Non-Cryst. Solids **172–174**, 1222 (1994).
[14] D. Ravaine and J. L. Souquet, Phys. Chem. Glasses **18**, 27 (1977).
[15] D. Ravaine and J. L. Souquet, Phys. Chem. Glasses **19**, 115 (1978).
[16] D. Ravaine, J. Non-Cryst. Solids **73**, 287 (1985).
[17] H. L. Tuller and D. P. Button, *Transport-Structure Relations in Fast Ion and Mixed Conductors*, edited by F. W. Poulsen, N. Hessel-Andersen, K. Clausen, S. Skaarup, and O. Soerensen (Risø National Laboratory, Roskilde, Denmark, 1985), p. 119.
[18] J. Swenson, L. Börjesson, and W. S. Howells, Phys. Rev. Lett. **77**, 3569 (1996).
[19] R. L. McGreevy and L. Pusztai, Mol. Simul. **1**, 359 (1988).
[20] St. Adams and J. Swenson, Phys. Rev. Lett. **84**, 4144 (2000).
[21] I. D. Brown, Acta Crystallogr., Sect. B: Struct. Sci. **B53**, 381 (1997); **B48**, 553 (1992).
[22] V. S. Urusov, Acta Crystallogr., Sect. B: Struct. Sci. **B51**, 641 (1995).
[23] K. Waltersson, Acta Crystallogr., Sect. A: Cryst. Phys., Diffr., Theor. Gen. Crystallogr. **A34**, 901 (1978).
[24] I. D. Brown, in *Structure and Bonding in Crystals*, edited by M. O'Keeffe and A. Navrotsky (Academic Press, New York, 1981), Vol. II, pp. 1–30.
[25] N. E. Brese and M. O'Keeffe, Acta Crystallogr., Sect. B: Struct. Sci. **B47**, 192 (1991).
[26] S. F. Radaev, L. Fink, and M. Trömel, Z. Kristallogr. Suppl. **8**, 628 (1994); M. Trömel (private communication).
[27] J. P. Naskar, S. Hati, and D. Datta, Acta Crystallogr., Sect. B: Struct. Sci. **B53**, 885 (1997).
[28] *International Tables of X-Ray Crystallography*, edited by A. J. C. Wilson (Kluwer, Dordrecht, 1992), Vol. C, p. 681.
[29] J. D. Garrett, J. E. Greedan, R. Faggiani, S. Carbotte, and I. D. Brown, J. Solid State Chem. **42**, 183 (1982).
[30] R. J. Cava, F. Reidinger, and B. J. Wuensch, Solid State Commun. **24**, 411 (1977).
[31] St. Adams, W. F. Kuhs, and D. Wilmers, Z. Kristallogr. Suppl. **16**, 87 (1999).
[32] St. Adams and A. Preusser, Acta Crystallogr., Sect. C: Cryst. Struct. Commun. **C55**, 1741 (1999).
[33] St. Adams and J. Maier, Solid State Ionics **105**, 67 (1998).
[34] R. Withers, S. Schmid, and J. G. Thompson, Prog. Solid State Chem. **26**, 1 (1998).
[35] St. Adams, K. H. Ehses, and J. Spilker, Acta Crystallogr., Sect. B: Struct. Sci. **B49**, 958 (1993).
[36] St. Adams, K. Hariharan, and J. Maier, Solid State Ionics **86–88**, 503 (1996).
[37] St. Adams, J.-S. Lee, and J. Maier, Mater. Struct. **5A**, 68 (1998).
[38] St. Adams, Solid State Ionics **136/7**, 1351 (2000).
[39] A. LeBail, J. Non-Cryst. Solids **183**, 39 (1995).
[40] St. Adams, Z. Kristallogr. **211**, 770 (1996).
[41] R. L. McGreevy, Annu. Rev. Mater. Sci. **22**, 217 (1992).
[42] R. L. McGreevy, Nucl. Instrum. Methods Phys. Res. A **354**, 1 (1995).
[43] N. Metropolis, A. W. Rosenbluth, M. N. Rosenbluth, A. H. Teller, and E. Teller, J. Phys. Chem. **21**, 1087 (1953).
[44] W. S. Howells, Rutherford-Appleton Laboratory Report No. RAL-86-042, 1986 (unpublished).
[45] G. Buchnell-Wye and R. J. Cernik, Rev. Sci. Instrum. **63**, 999 (1992).
[46] D. A. Keen, Phase Transit. **61**, 109 (1997).
[47] C. Chiodelli, A. Magistris, M. Villa, and J. L. Bjorkstam, J. Non-Cryst. Solids **51**, 143 (1982).
[48] V. M. Neild, D. A. Keen, W. Hayes, and R. L. McGreevy, Solid State Ionics **66**, 247 (1993).

[49] J. Swenson, R. L. McGreevy, L. Börjesson, and J. D. Wicks, J. Phys.: Condens. Matter **8**, 3545 (1996).
[50] J. Swenson, L. Börjesson, R. L. McGreevy, and W. S. Howells, Phys. Rev. B **55**, 11 236 (1997).
[51] J. Swenson, L. Börjesson, and W. S. Howells, J. Phys.: Condens. Matter **11**, 9275 (1999).
[52] J. Swenson and St. Adams (unpublished).
[53] A. Karthikeyan and K. J. Rao, J. Phys. Chem. B **101**, 3105 (1997).
[54] M. D. Ingram, Curr. Opin. Solid State Mater. Sci. **2**, 399 (1997).
[55] J. Swenson, R. L. McGreevy, L. Börjesson, and J. D. Wicks, Solid State Ionics **105**, 55 (1998).
[56] J. Wicks, L. Börjesson, R. L. McGreevy, W. S. Howells, and G. Bushnell-Wye, Phys. Rev. Lett. **74**, 726 (1995).
[57] M. D. Ingram, Phys. Chem. Glasses **25**, 215 (1987).
[58] N. Zotov and H. Keppler, Phys. Chem. Miner. **25**, 259 (1998); N. Zotov (private communication).
[59] A. Kvist and A.-M. Josefson, Z. Naturforsch. A **23A**, 625 (1968).
[60] J. Kawamura and M. Shimoji, J. Non-Cryst. Solids **88**, 281 (1986).
[61] M. C. R. Shastry and K. J. Rao, Solid State Ionics **37**, 17 (1989).
[62] C. A. Angell, Solid State Ionics **18–19**, 72 (1986).
[63] G. Chiodelli, G. Campari Vigano, G. Flor, A. Magistris, and M. Villa, Solid State Ionics **8**, 311 (1983).
[64] A. Schiraldi and E. Pezzati, Mater. Chem. Phys. **23**, 75 (1989).
[65] G. Carini, M. Cutroni, M. Federico, G. Galli, and G. Tripodo, Phys. Rev. B **30**, 7219 (1984).
[66] K. Sebastian and G. H. Frischat, Phys. Chem. Glasses **33**, 199 (1992).
[67] T. Minami, Y. Ikeda, and M. Tanaka, J. Non-Cryst. Solids **52**, 159 (1982).
[68] A. Magistris, G. Chiodelli, and A. Schiraldi, Electrochim. Acta **24**, 203 (1979).
[69] St. Adams, habilitation thesis, Göttingen, 2000.
[70] M. Sayer, S. L. Segel, J. Noad, J. Corey, T. Boyle, R. D. Heyding, and A. Mansingh, J. Solid State Chem. **42**, 191 (1982).
[71] M. N. Avashti, M. Saleem, and M. T. El-Gemal, Solid State Ionics **6**, 43 (1982).
[72] W. Meyer and H. Neldel, Z. Tech. **18**, 588 (1937).